Ultra-wideband Electrical Sensing of Nucleus Size in a Live Cell

Xiaotian Du, Caroline Ladegard, Xiao Ma, Xuanhong Cheng, James C. M. Hwang Lehigh University, Bethlehem, PA 18015, USA xid415@lehigh.edu

Abstract — Recently, ultra-wideband electrical sensing has been developed as a fast, compact, and label-free technique to characterize a biological cell noninvasively and to extract its intracellular properties. This paper presents, for the first time, the use of the technique to sense the change in the nucleus size of a live Jurkat cell. The experiment is based on trapping and detrapping the cell by dielectrophoresis on a coplanar waveguide and measuring the return and insertion losses due to the presence of the cell from 9 kHz to 9 GHz. The results have been validated by traditional fluorescence microscopy. In the future, by extending the technique to detect changes in nucleus shape and DNA content, it could be used to distinguish cancerous cells from normal cells, for example.

Keywords — Biological cells, biosensors, Nuclear measurements, microwave measurements, ultra wideband technology.

I. INTRODUCTION

Morphological and structural changes of a cell nucleus and its DNA content are well-known screening, diagnostic and prognostic markers in cancer cytology [1]. Currently, abnormalities in nuclear morphology are mostly determined through optical microscopy and flow cytometry, which usually require cell labeling and, hence, are invasive and labor intensive [2]. On the other hand, advanced nano-electrodes that penetrate into cells have been used to reveal properties of intra-cellular organelles [3], [4], but are even more invasive and difficult to standardize or scale up.

Recently, single-cell electrical sensing at microwave frequencies has been developed, taking advantage of the ability of the microwave signal to penetrate into a cell noninvasively [5], [6]. Using such a fast, compact and label-free technique, intra-cellular dielectric properties can be obtained accurately and reproducibly. Most recently, using an ultra-wideband (UWB) vector network analyser (VNA), single-cell sensing can be conveniently accomplished from kilohertz to gigahertz frequencies, so that both the whole-cell and intra-cellular properties are simultaneously obtained [7], [8]. This paper focuses on the use of UWB electrical sensing of the nucleus size in a live cell as illustrated in Fig. 1.

II. EXPERIMENTAL PROCEDURE

A. Cell Preparation

For proof of principle, Jurkat human lymphocyte cells were chosen for their large size, simple structure, and nonadherent nature. The cells were cultured in Sigma-Aldrich RPMI 1640 with 10% fetal bovine serum, 100 units/mℓ penicillin, and 100

μg/mℓ streptomycin under 37 °C and 5% CO₂. The cultured cells were twice washed and re-suspended in an isotonic solution of 8.5% sucrose and 0.3% dextrose to a concentration of 3 × 106 cell/mℓ for electrical sensing. Cell viability was verified in a separate experiment with Trypan Blue dye, which showed more than half of cells survived after 10 h [6]. To artificially shrink the nucleus size, different batches of cells were treated with a solution of 460 μg/mℓ staurosporine in dimethyl sulfoxide (DMSO) for 1, 2, or 3 h [9]. Untreated cells were kept as a control. All cells were then washed and resuspended in fresh media before undergoing optical or electrical measurement.

B. Optical Measurement

Fluorescent staining was used to ensure the measured electrical signal reflects change in the nucleus size rather than the cell size. To this end, cells were moved to a medium containing only RPMI 1640 and stained by 4 μ g/m ℓ Hoechst 33342 in DMSO and 2 μ g/m ℓ Calcien-AM in DMSO for 30 min. Fig. 2(a) shows that the blue fluorescence by Hoechst 33342 indicates the nucleus size, whereas the green fluorescence by Calcien-AM indicates the cell size as well as cell viability. Optical micrographs were taken under different

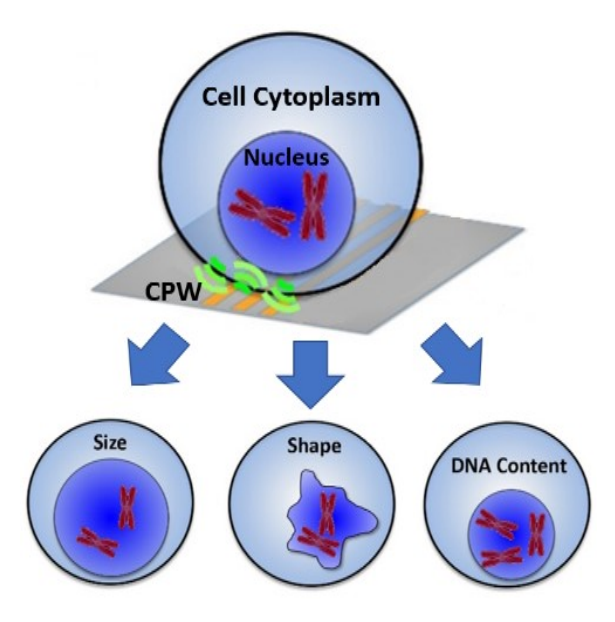
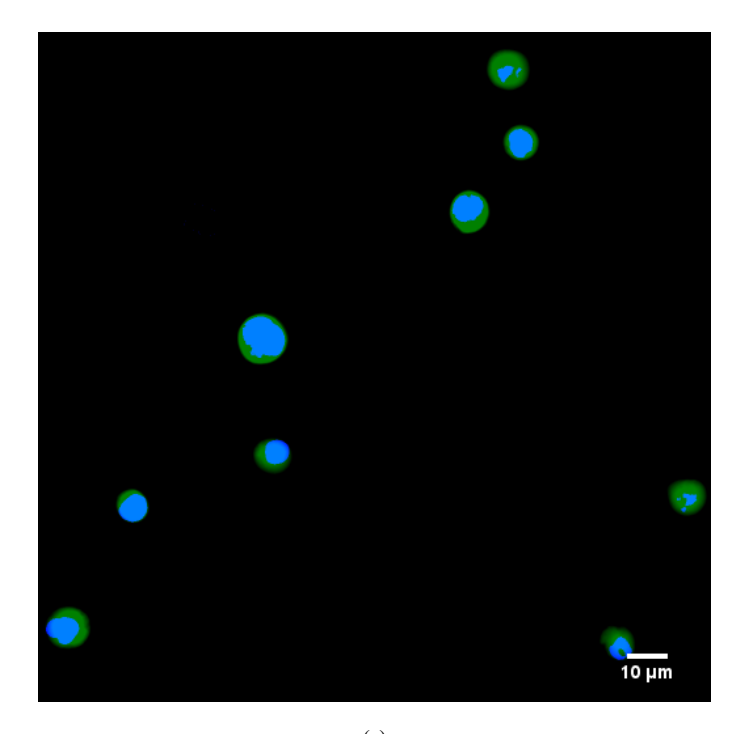


Fig. 1. Schematic illustration of ultra-wideband electrical sensing of a live cell on a coplanar waveguide for different nuclear morphology and DNA content.



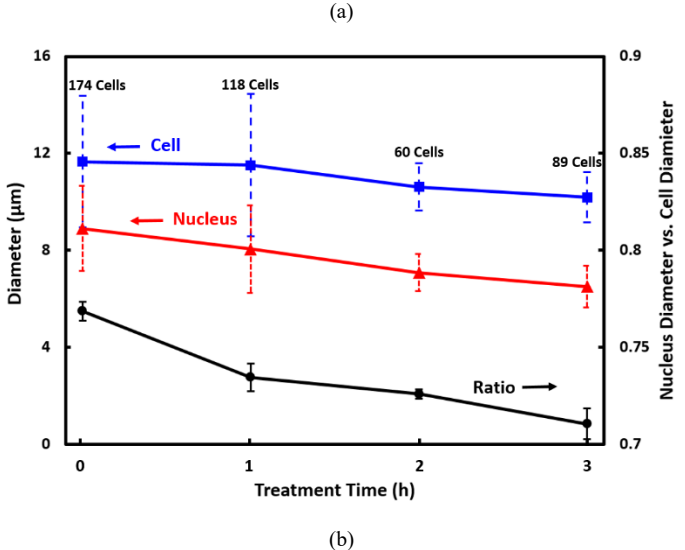
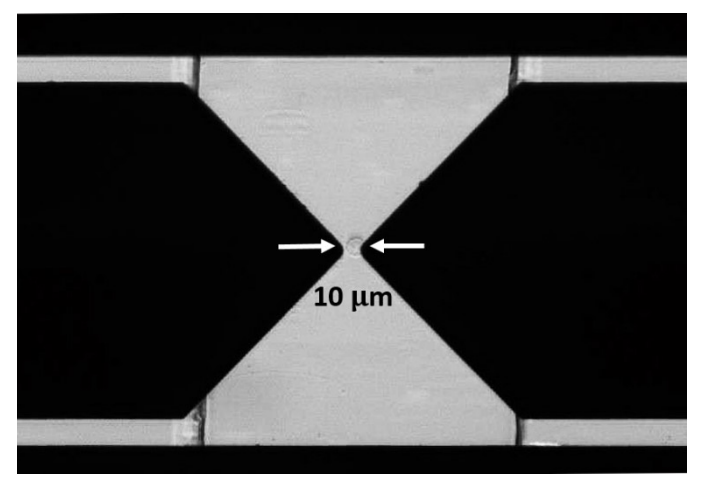


Fig. 2. (a) Fluorescent micrograph of cells stained with blue and green dyes reflecting nucleus and cell sizes, respectively. (b) Cell and nucleus diameters of cells treated with staurosporine for 0, 1, 2 and 3 h, respectively.

fluorescence settings and analyzed statistically using the ImageJ program. Altogether, the statistics involved 174, 118, 60, and 89 cells treated in staurosporine for 0, 1, 2, and 3 h, respectively. Fig. 2(b) plots the cell and nucleus diameters as a function of treatment time. It can be seen that, although both the cell and nucleus shrink with increasing treatment time, they ratio decreases monotonically, too.

C. Electrical Measurement

Altogether twelve different electrical measurements were performed on twelve different cells using two UWB coplanar waveguides (CPWs) with a series or shunt trap for a cell as shown in Fig. 3(a) and Fig. 3(b), respectively. The series and



(a)

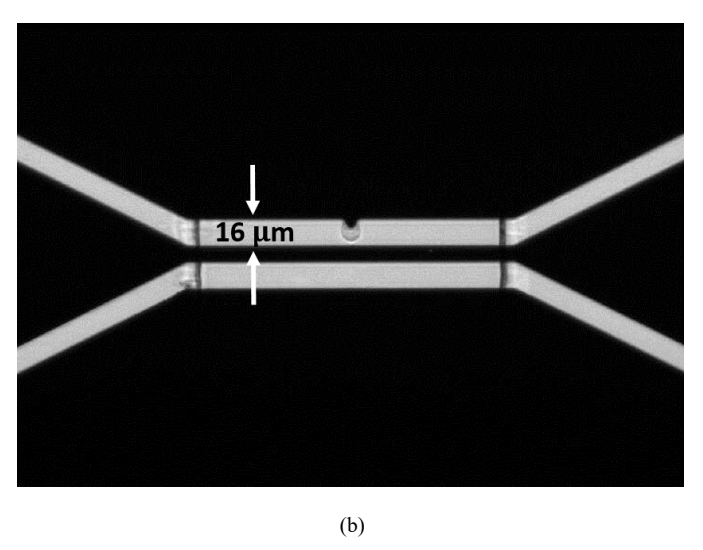


Fig. 3. Micrographs of a live Jurkat cell trapped in a (a) series or (b) shunt configuration on a coplanar waveguide for electrical measurement.

shunt configurations are complementary in extracting the different characteristics of intra-cellular compartments [10]. Six cells were characterized in the series configuration; another six were characterized in the shunt configuration. Each set of six measurements involved three cells treated in staurosporine for 3 h and three untreated cells. Bright-field micrographs were taken simultaneous to the electrical measurements to ensure there was no systematic difference in the overall size between treated and untreated cells chosen for electrical sensing. Specifically, the treated and untreated cells used in the series configuration had diameters of 11.8 \pm 0.3 μm and 12.1 \pm 0.3 μm, respectively. For the shunt configuration, the treated and untreated cells had diameters of $13.5 \pm 0.4 \mu m$ and 13.2 ± 0.3 μm, respectively. Thus, the differences were within the measurement uncertainties and the measured electrical signal should reflect change in the nucleus size rather than the cell size.

Similar to [7], the present test setup is based on a homemade microwave probe station on a Nikon Eclipse Ti-E inverted fluorescence microscope. The device under test comprises a 1-cm-long and 0.5-µm-thick gold CPW sandwiched between a

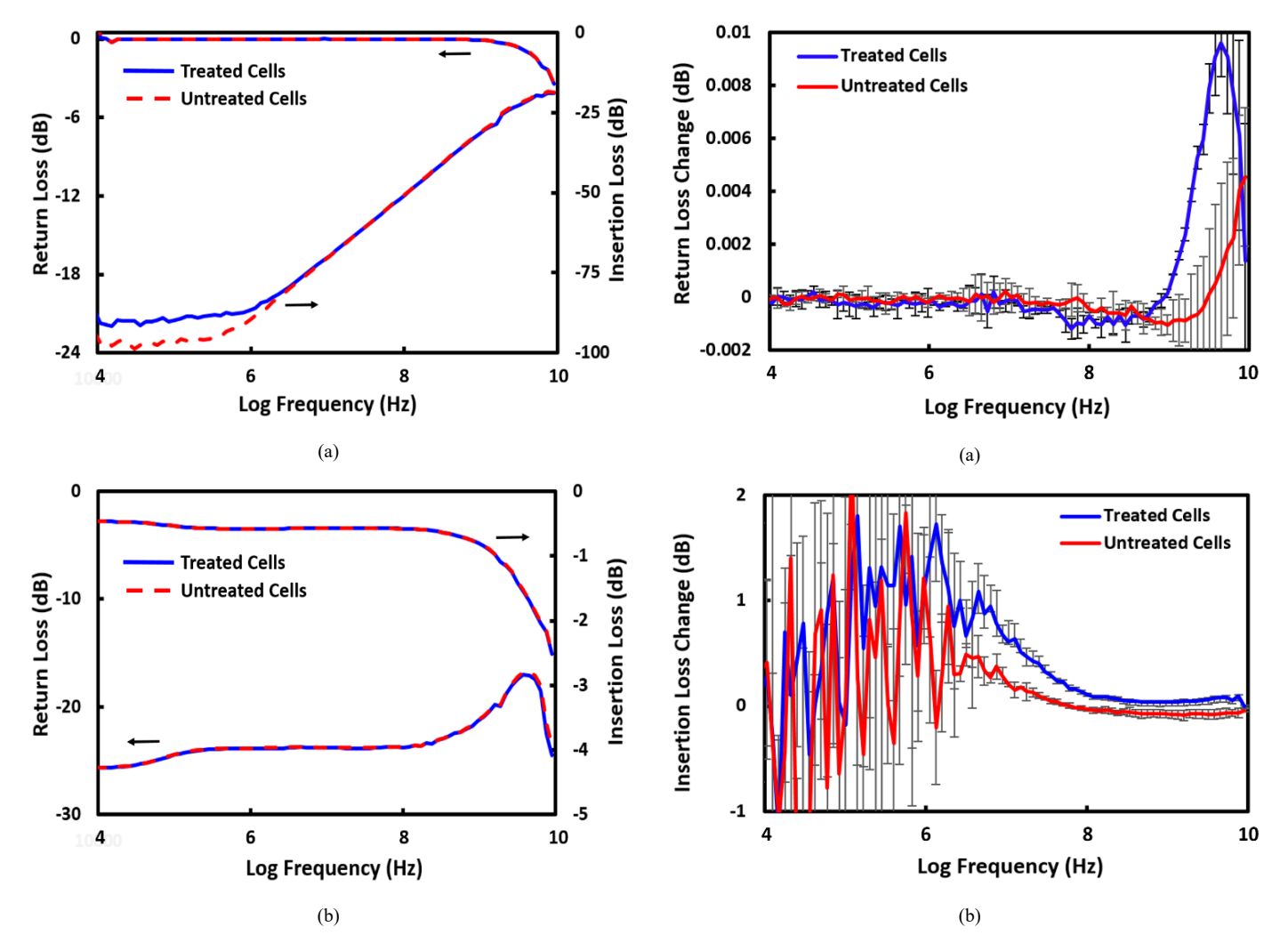


Fig. 4. Measured return loss and insertion loss in (a) series configuration and (b) shunt configuration, respectively.

0.5-mm-thick quartz substrate and 5-mm-thick polydimethylsiloxane (PDMS) cover etched on its underside with a 5-mm-long, 200-μm-wide, and 20-μm-deep microfluidic channel. The PDMS cover intersected the CPW perpendicularly. The gap between the center and ground electrodes of the CPW is 16 µm. For the series configuration, the center electrode is mostly 200-µm wide except under the microfluidic channel, where it is tapered down to a 10 µm by 10 µm gap as shown in Fig. 3(a). For the shunt configuration, the center electrode is tapered to 10 µm uniformly under the microfluidic channel, while one of the ground electrodes includes a 6-µm protrusion in the middle reducing the gap size to 10 µm as shown in Fig.

For electrical measurements, suspensions of both treated and untreated cells according to Sec. IIA were injected through the microfluidic channel at approximately 0.1 $\mu\ell/min$ as controlled by a syringe pump. For each electrical measurement, continuous waves of -15 dBM from 9 kHz to 9 GHz generated by a Keysight Technologies E5080A VNA was applied to the CPW via a pair of Cascade Microtech ACP40 GSG 200- μ m-pitched probes. Before the electrical measurement, a 3-dBm, 5-

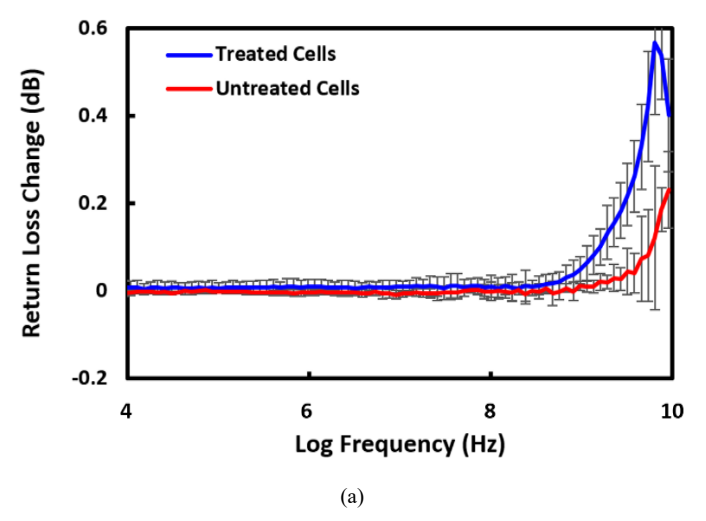
Fig. 5. Measured changes in (a) return loss and (b) insertion loss for staurosporine-treated and untreated cells in *series* configuration.

MHz signal was generated by the same VNA to trap the cell on the CPW by positive dielectrophoresis. After the electrical measurement, a 3-dBm,10-kHz signal was generated by the same VNA to detrap the cell by negative dielectrophoresis. Rapidly consecutive scattering parameters in terms of return and insertion losses were measured with and without the cell, and the difference due to the presence of the cell was calculated and recorded. This helps mediate the effect of a drifting background on the small (~ 0.001 dB) difference of the signal due to the presence of a call, as in the case of interferometer measurement [10].

III. RESULTS AND DISCUSSION

Fig. 4(a) and (b) show well-behaved and spurious-free UWB return and insertion losses, in series and shunt configurations, respectively. Notable exception is in the insertion loss in the series configuration at 1 MHz or lower where the signal is below the noise floor.

Fig. 5 shows changes in return and insertion losses due to a cell trapped in *series* configuration. Despite the small and scattered data, systematic difference exists between treated and



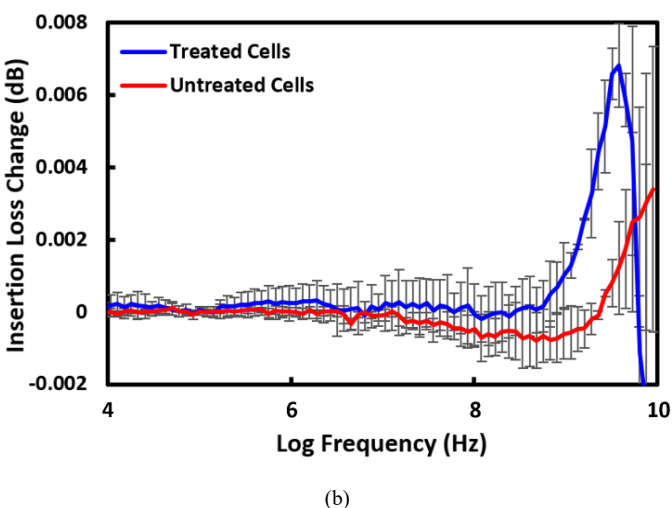


Fig. 6. Measured changes in (a) return loss and (b) insertion loss for staurosporine treated and untreated cells in *shunt* configuration.

untreated cells. It can be seen in Fig. 5(a) that the difference in return loss occurs mainly at gigahertz frequencies and the peak change shifts from approximately 4.5 GHz for treated cells to above 9 GHz for untreated cells. It can be seen in Fig. 5(b) that the difference in insertion loss occurs across the band, except at 1 MHz or below where the signal is below the noise floor.

Fig. 6 shows changes in return and insertion losses due to a cell trapped in *shunt* configuration. Again, despite the small and scattered data, systematic difference exists between treated and untreated cells. It can be seen that the difference increases with increasing frequency and the peak change shifts to higher frequencies for untreated cells. From these measured changes in electrical characteristics, modeling and analysis are in progress to extract the size and permittivity of the nucleus vs. that of the cell.

IV. CONCLUSIONS

UWB electrical sensing was found capable of detecting changes in the nucleus size of live Jurkat cells. Changes in terms of microwave return and insertion losses occur across the band

and peak at different frequencies. Such frequency dispersion could be used to extract the nucleus size and permittivity noninvasively. Additionally, with more detailed measurement and analysis, we should be able to extract the nucleus shape and DNA content, which could be used to distinguish, e. g., cancerous cells from normal cells.

Historically, electrical cell sensing has been referred to as impedance spectroscopy or dielectric spectroscopy. Whereas cell impedance can be directly extracted from the measured return or insertion losses, cell permittivity can only by inferred with assumptions of cell size and shape. This is even more challenging in separating the permittivities of different cell compartments. To this end, the present result suggests that UWB impedance spectroscopy can be used to extract directly morphological information, e. g., cell size at low frequencies and nucleus size at high frequencies. This can serve as the first step towards separating the permittivities of the cytoplasm from that of the nucleus.

ACKNOWLEDGMENT

This work was supported in part by the U.S. National Science Foundation under Grant ECCS-1809623, Army Research Office under Grant W911NF-14-1-0665, and Air Force Office of Scientific Research under Grant FA9550-16-1-0475.

REFERENCES

- [1] P. Jevtic, L. J. Edens, L. D. Vukovic, and D. L. Levy, "Sizing and shaping the nucleus: mechanisms and significance," *Curr. Opin. Cell Biol.*, vol. 28, pp. 16–27, Jun. 2014.
- [2] M. A. Al-Abbadi, "Basics of cytology," Avicenna J. Med., vol. 1, no. 1, pp. 18–28, Jul.-Sep. 2011.
- [3] M. Kang, S. Jung, H. N. Zhang, T. Kang, H. Kang, Y. Yoo, J. P. Hong, J. P. Ahn, J. Kwak, D. Jeon, N. A. Kotov, and B. Kim, "Subcellular neural probes from single-crystal gold nanowires," ACS Nano, vol. 8, no. 8, pp. 8182–8189, Aug. 2014.
- [4] A. M. Xu, A. Aalipour, S. Leal-Ortiz, A. H. Mekhdjian, X. Xie, A. R. Dunn, C. C. Garner, and N. A. Melosh, "Quantification of nanowire penetration into living cells," *Nat. Comm.*, vol. 5, no. 4613, pp. 1–8, Apr. 2014.
- [5] T. Chen, F. Artis, D. Dubuc, J.-J. Fournie, M. Poupot, and K. Grenier, "Microwave biosensor dedicated to the dielectric spectroscopy of a single alive biological cell in its culture medium," in *IEEE MTT-S Int. Microwave Symp. (IMS) Dig.*, Jun. 2013, pp. 1–4.
- [6] Y. Ning, C. Multari, X. Luo, C. Palego, X. Cheng, J. C. M. Hwang, A. Denzi, C. Merla, F. Apollonio, and M. Liberti, "Broadband electrical detection of individual biological cells," *IEEE Trans. Microw. Theory Techn.*, vol. 62, no. 9, pp. 1905–1911, Sep. 2014.
- [7] X. Ma, X. Du, H. Li, X. Cheng, and J. C. M. Hwang, "Ultra-wideband impedance spectroscopy of a live biological cell," *IEEE Trans. Microw. Theory Techn.*, vol. 66, no. 8, pp. 3690–3696, Aug. 2018.
- [8] X. Du, X. Ma, L. Li, H. Li, X. Cheng, and J. C. M. Hwang, "Validation of Clausius-Mossotti function in wideband single-cell dielectrophoresis," *IEEE J. Electromagn. RF Microw. Med. Bio.* Available: http://doi/ 10.1109/JERM.2019.2894100.
- [9] I. Chowdhury, W. Xu, J. K. Stiles, A. Zeleznik, X. Yao, R. Matthews, K. Thomas, and W. E. Thompson, "Apoptosis of rat granulosa cells after staurosporine and serum withdrawal is suppressed by adenovirus-directed overexpression of prohibition," *Endocrinology*, vol. 148, no. 1, pp. 206–217, Jan. 2007.
- [10] X. Ma, X. Du, L. Li, H. Li, X. Cheng, and J. C. M. Hwang, "Sensitivity analysis for ultra-wideband 2-port impedance spectroscopy of a live cell," *IEEE J. Electromagn. RF Microw. Med. Biol.* Submitted for publication.